Transient Event Detection for Nonintrusive Load Monitoring and Demand Side Management Using Voltage Distortion

Robert Cox and Steven B. Leeb
Laboratory for Electromagnetic and Electronic Systems
Massachusetts Institute of Technology
Cambridge, MA 02139
Email: rwcox@mit.edu, sbleeb@mit.edu

Steven R. Shaw
Department of Electrical and Computer Engineering
Montana State University
Bozeman, MT

Leslie K. Norford
Department of Architecture
Massachusetts Institute of Technology
Cambridge, MA 02139
Email: lnorford@mit.edu

***Abstract*— This paper describes a simple system that can be used for autonomous demand-side management in a load site such as a home or commercial facility. The system identifies the operation of individual loads using transient patterns observed in the voltage waveform measured at an electric service outlet. The theoretical foundation of the measurement process is introduced, and a preprocessor that computes short-time estimates of the spectral content of the voltage waveform is described. The paper presents several example measurements demonstrating the ability of the system to obtain estimates of the spectral content of the voltage waveform.**

I. Introduction

Recent estimates indicate that products containing power supplies consume over 200 billion kWh of energy each year in the United States [1]. Additionally, market projections suggest that this number will grow over time, as worldwide sales of power supplies are expected to grow approximately 15% each year [1]. With so much energy consumed by power electronic circuits, it is clear that one way to effect a significant reduction in peak energy consumption at a load site such as a home or commercial facility is to introduce autonomous demand-side energy management features. For example, the control circuitry included in switching power supplies could incorporate a consumption control feature that would place the device in a low power mode following the detection of the operation of a large energy consumer such as an electric water heater. This paper describes a potentially inexpensive system that could allow a device to sense the operation of other loads on the local utility distribution network using measurements of the local utility voltage.

The method used here to identify the operation of individual loads is based on the observation that the transient behavior of an electrical load is strongly influenced by the task that the load performs [2]. Consequently, different classes of loads posses unique and repeatedly observable transient profiles that can serve as "fingerprints" indicating the operation of individual loads. For instance, the turn-on transients associated with an incandescent lamp and an induction motor are distinctly different, as the physical task of heating the cold filament of a lamp is not the same as accelerating a rotor [2]. That concept has been used to develop a device known as the nonintrusive load monitor (NILM) that can detect the operation of individual loads using transient patterns observed in the short-time estimates of the spectral content of the aggregate current drawn by a collection of loads [2], [3]. The prototype system described in this paper takes the nonintrusive monitoring concept one step further by identifying load operation using the voltage distortion caused by transient load currents.

The paper begins in Section II by introducing the concepts that motivate nonintrusive load monitoring and by describing the theoretical background upon which the current system is based. Section III describes both the continuous-time and discrete-time operations performed by the preprocessor that computes estimates of the spectral content of the measured voltage waveform. Additionally, Section III also provides numerous examples that demonstrate the ability of the preprocessor to sense the small changes in the voltage waveform that are the result of individual load currents. Section IV provides a description of the methods used by the prototype system to identify the operation of individual loads, and it also includes several examples that demonstrate the success of the load identification scheme. Finally, the paper concludes in Section V by summarizing the results and by describing several areas of ongoing research.

II. Spectral Envelope Estimation

In standard approaches to nonintrusive monitoring, loads are detected using the two step procedure shown in Fig. 1 [2], [3]. In the first step, a preprocessor, which can be implemented using either analog electronics or digital software routines, computes estimates of the short-time spectral content of a measured current waveform [2]–[4]. Subsequently, the spectral estimates created by the preprocessor are passed to a software module that identifies the operation of individual loads by matching stored templates to transient patterns observed in the preprocessed data stream [3].

0-7803-9547-6/06/$20.00 ©2006 IEEE.

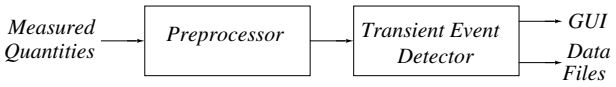

Fig. 1. System level block diagram of a typical nonintrusive load monitoring device. In each of the various incarnations of the traditional NILM, the measured quantities are the line voltage and the aggregate current flowing to a collection of loads [2], [3]. The system described in this paper uses a similar overall architecture, but its only input is the voltage measured at a single electric service outlet.

The preprocessor found in most nonintrusive monitoring devices performs a spectral decomposition of the current, $i(t)$, that is drawn by a collection of loads [2]–[4]. That procedure is based on the fact that a real waveform $x(t)$ may be described with arbitrary accuracy at time $t \in (t-T, t]$ by a Fourier series with time-varying, real spectral coefficients $a_k(t)$ and $b_k(t)$:

$$x\left(t-T+s\right) = \sum_k a_k(t)\cos(k\frac{2\pi}{T}(t-T+s)) + \sum_k b_k(t)\sin(k\frac{2\pi}{T}(t-T+s)). \quad (1)$$

In Eq. 1 the variable k ranges over the set of non-negative integers, T is a real period of time, and $s \in (0, T]$ [2], [5]. The coefficients $a_k(t)$ and $b_k(t)$ are calculated using the following formulae [5]:

$$a_k(t) = \frac{2}{T}\int_0^T x(t-T+s)\cos(k\frac{2\pi}{T}(t-T+s))ds \quad (2)$$

and

$$b_k(t) = \frac{2}{T}\int_0^T x(t-T+s)\sin(k\frac{2\pi}{T}(t-T+s))ds. \quad (3)$$

In a traditional NILM with access to both voltage and current measurements, estimates of the spectral coefficients $a_k(t)$ and $b_k(t)$ for the current $i(t)$ are created by synchronizing the function $\cos\left(\frac{2\pi}{T}t\right)$ in Eq. 2 with the local utility voltage and then averaging the products of the observed current and the synchronized sine waves over one or more periods of the measured voltage [2], [3]. Thus, a traditional NILM requires measurements of both the current and the voltage at the aggregate measurement point.

Figure 2 shows spectral estimates created by the preprocessor described in [4]. The waveforms in Fig. 2 correspond to the in-phase fundamental components of the currents drawn by an incandescent light bulb (top trace) and by a fractional horsepower induction motor (bottom trace). Superimposed on top of both spectral envelope waveforms is an identification template that was fit to the observed transient patterns by event detection software [3].

The preprocessor included in the prototype system presented in this paper requires only voltage measurements. Specifically, the preprocessor described here computes spectral envelope estimates of the voltage measured at a single electric service outlet. The development of this system demonstrates

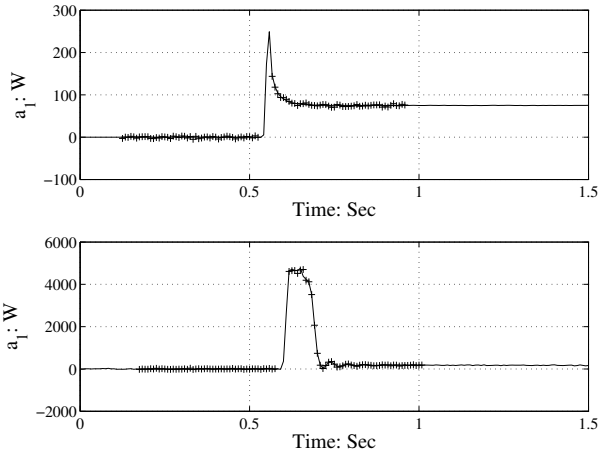

Fig. 2. Estimates of the spectral coefficient $a_1(t)$ as produced by the nonintrusive monitoring device described in [4]. The upper trace shows the estimate during the start of an incandescent lamp, and the bottom trace shows the estimate during the start of single-phase induction motor. Also shown in each plot is the template that has been properly matched to the observed transient behavior by the load identification software described in [3]. Note that the y-axes are labeled in units of Watts. Such labelling is customary in a traditional NILM, as the spectral coefficient $a_1(t)$ corresponds to a quantity that is proportional to real or "time average" power [2].

that nonintrusive load monitoring and event detection can be performed without a current sensor, making monitoring as easy as plugging in an appliance.

The monitoring approach described in this paper is based on the utility model shown in Fig. 3. In that model, we assume that electrical loads are connected to the secondary of a transformer that is driven at its primary by a stiff AC voltage source. With certain simplifying assumptions, the resistance R_s and the inductance L_s represent the composite impedances of cabling, protection circuitry, and the dominant transformer in the service stream. The resistances R_k and the inductances L_k represent the impedances of individual branch circuits that are fed from the transformer secondary. Physically, for example, the branch circuits shown in Fig. 3 might correspond to individual circuits in a home. Numerous researchers have found this model to be reasonably accurate provided that one considers a relatively limited frequency range that includes a limited number of low order harmonics of the fundamental power system frequency [6]–[9]. In fact, the authors of [6] and [7] used this model to estimate the impedance of the local distribution network for frequencies extending to about the 15^{th} harmonic of 60Hz.

The preprocessor used in the current system is supplied with measurements of the voltage observed at a single service outlet. For example, the preprocessor might measure one of the voltages $v_k(t)$ shown in Fig. 3. Whenever a load is either connected to or disconnected from one of the terminals shown in the figure, the voltage at the measurement node, which we denote as $v_m(t)$, will change as a result of the harmonic currents that are drawn through R_s and L_s. For example, Fig. 4 shows the line voltage measured at one outlet in an apartment

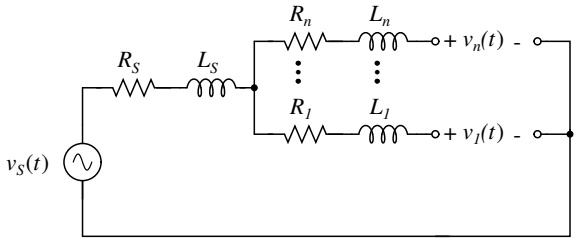

Fig. 3. A distribution-level model of the electric utility.

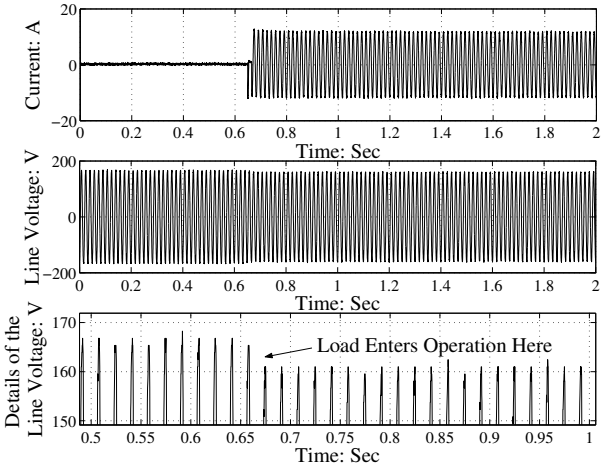

Fig. 4. Distortion in the measured line voltage as a result of the connection of a 1kW heater. The top trace shows the load current drawn by the heater (for reference), the middle trace shows the line voltage applied to the heater, and the bottom trace shows the details near the peak of the line voltage.

both before and after the connection of a 1kW heater at another outlet in the same apartment. Note that the amplitude of the voltage waveform changes immediately following the connection of the load.

As demonstrated in Fig. 4, the measured line voltage contains a component that is a scaled and time shifted replica of the load current. Given that transient patterns observed in the spectral content of the load current can be used to identify the operation of individual loads, transient patterns observed in the spectral content of the measured voltage can be used in a similar manner. The relatively small change in the utility voltage is the primary challenge in designing a preprocessor that extracts transient profiles from the measured voltage waveform. The development of a voltage-only preprocessor is discussed in the next section.

III. Spectral Envelope Preprocessor Implementation

In the preprocessor prototype, a set of spectral coefficients denoted as $a_{k,AN}(t)$ and $b_{k,AN}(t)$ are computed using the synchronous detection scheme that is outlined in block diagram

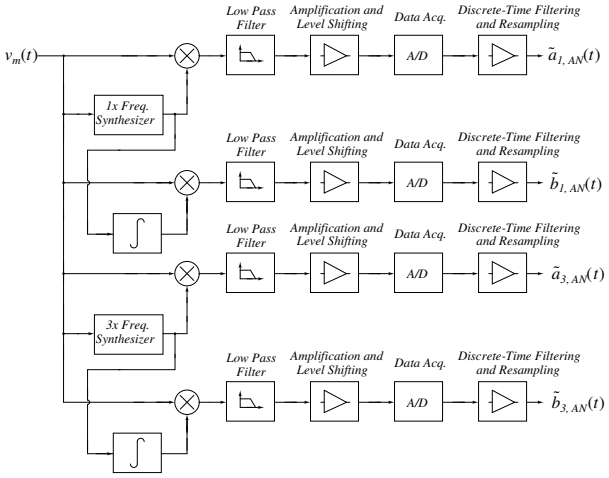

Fig. 5. Block diagram of the spectral envelope preprocessor used in the current system. The frequency synthesizers are constructed using phase-locked loops. The amplification and level-shifting circuitry following the low pass filters is required in order ensure that the output signals are within the range of the A/D converter in the data acquisition system. Note that the two integrators in this system are used to shift the appropriate reference waveforms by 90^o.

form in Fig. 5.[1] In that system, several analog frequency synthesizers generate reference waveforms that are phase-locked to the voltage measured between the "hot" wire and the neutral wire at a single service outlet. These waveforms are then input to a set of analog multipliers. One of the frequency components that results from multiplying each reference waveform with the measured line voltage is a slowly-varying, baseband term that is related to the appropriate spectral coefficient of the voltage. The multiplier outputs are passed to second order low pass filters that reduce unwanted high frequency content. The filter outputs are level shifted and slightly amplified prior to their conversion into the discrete-time domain. Once quantized, the output of each channel shown in Fig. 5 is numerically integrated over a sliding window using a trapezoidal approximation. That operation significantly reduces any remaining high frequency content and produces high quality estimates of the spectral coefficients $a_{k,AN}(t)$ and $b_{k,AN}(t)$. In order to ease computational burdens, the final outputs are slightly downsampled.

For a number of different loads, estimates of the spectral coefficient $a_{1,AN}(t)$ are reliable and repeatable indicators of the load operation. For instance, Fig. 6 shows the behavior observed during the start of a 1kW heater.[2] Since this load is

[1]For $k = 1$, the coefficients $a_{k,AN}(t)$ and $b_{k,AN}(t)$ are roughly analogous to real and reactive power, respectively. Additionally, $a_{k,AN}(t)$ and $b_{k,AN}(t)$ are also measures of in-phase and quadrature voltage distortion, respectively.

[2]The scales on the y-axes of all of the spectral estimate plots shown from Fig. 6 onward correspond to the scales of the voltages measured at the outputs of the analog measurement circuits (i.e. at the inputs to the A/D converters). In order to determine the exact amount of line distortion, each of the plots shown here would need to be appropriately scaled. Additionally, the plots of the spectral estimates are labeled as in-phase or quadrature voltage distortion. In this case, the a_k are considered to be measures of the in-phase voltage distortion, and the b_k are considered to be measures of quadrature voltage distortion.

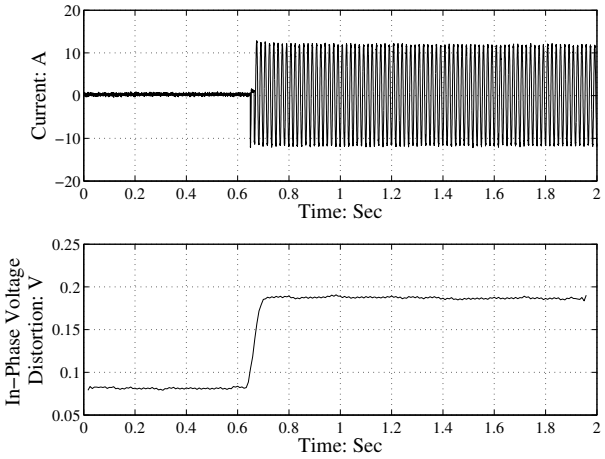

Fig. 6. The measured load current (for reference) and the measured estimate of $a_{1,AN}(t)$ during the start of a 1kW heater. Note that the estimate of $a_{1,AN}(t)$ is labeled as in-phase voltage distortion.

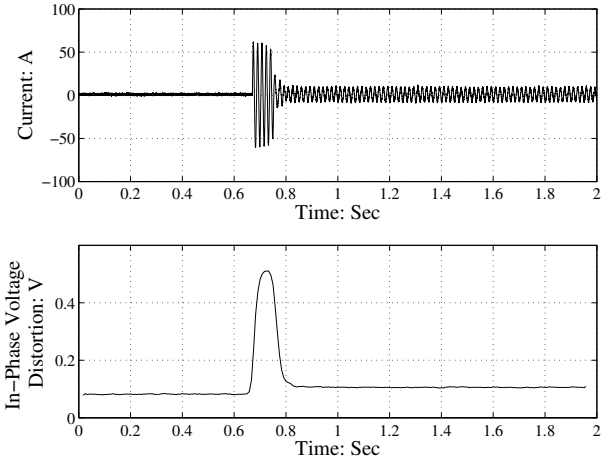

Fig. 7. The measured load current (for reference) and the measured estimate of $a_{1,AN}(t)$ during the start of an unloaded, $1/3$hp, single-phase induction motor.

well approximated as a pure resistance, the real power that it draws should approximate a step function. This is the behavior observed in Fig. 6. A similar trend is observed in Fig. 7 for an unloaded, $1/3$hp single phase induction motor. In this case, $a_{1,AN}(t)$ is quite large during the transient period when the rotor is accelerating, and the steady state change is quite small. This behavior is expected, as an unloaded induction motor consumes minimal real power in steady operation.

As shown in Fig. 5, the procedure used to estimate $b_{1,AN}(t)$ is similar to that used to estimate $a_{1,AN}(t)$. The oscillator voltage is shifted by 90^o when estimating $b_{1,AN}(t)$. There is an important caveat to be noted when estimating $b_{1,AN}(t)$ in this way, however. Since the phase-locked frequency synthesizer must eventually synchronize to the new zero crossings of the voltage waveform, the overall steady state change in the

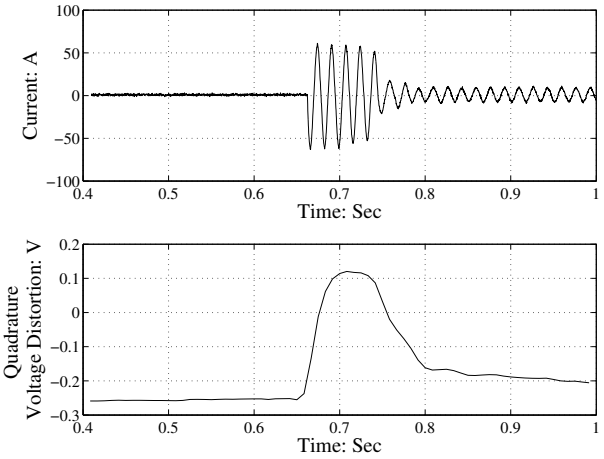

Fig. 8. Line current (for reference) and the estimate of $b_{1,AN}(t)$ during the start of an unloaded, $1/3$hp, single-phase induction motor. Note that the estimate of $b_{1,AN}(t)$ initially shows a very large change, but that the difference ultimately begins to decrease.

estimated value of $b_{1,AN}(t)$ should be zero. Thus, the estimate that is calculated by the prototype preprocessor is only valid for a short time following a transient event. This is reasonable, however, given that the goal of our system is to identify the operation of individual loads from their transient behavior.

Figure 8 displays the estimate of $b_{1,AN}(t)$ during the start of an unloaded, $1/3$hp, single-phase induction motor. As expected, the initial estimate is quite reasonable. As the motor enters steady state conditions, however, the estimate begins to decay. The amount of time for which the estimate remains valid is largely a function of the dynamics of the phase-locked loop in the frequency synthesizer. The difference between the estimated value of $b_{1,AN}(t)$ immediately before the motor start and the estimated value immediately following the end of the transient in-rush period is larger than the corresponding change observed in $a_{1,AN}(t)$ during the start of the same unloaded motor (see Fig. 7). This result is logical, as an unloaded induction motor mainly draws reactive power.

In addition to the load information that can be obtained by estimating the spectral coefficients of the line-to-neutral voltage at a single service outlet, it is also possible to extract information by estimating the spectral coefficients of the voltage measured between the neutral conductor and ground. That voltage, which we denote as $v_{NG}(t)$, also contains components that are related to the harmonic currents drawn by individual loads, as load currents return through the impedances of the neutral conductors. In our prototype, the spectral coefficients of the neutral-to-ground voltage are estimated using a measurement procedure similar to that used to estimate the spectral coefficients of the line-to-neutral voltage. Fig. 9 shows a block diagram of the components used to estimate $a_{1,NG}(t)$. That coefficient corresponds to the component of $v_{NG}(t)$ that is in-phase with the line-to-neutral voltage. Other coefficients are computed in a similar manner.

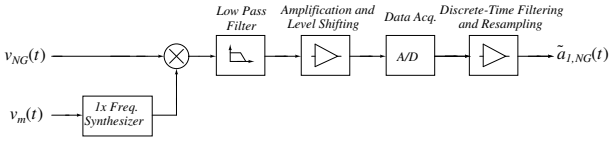

Fig. 9. Block diagram of the spectral envelope preprocessor used to estimate the spectral coefficient $a_{1,NG}(t)$ of the neutral-to-ground voltage. The voltage $v_m(t)$ that is input to the frequency synthesizer is the measured line-to-neutral voltage. Similar methods are used to estimate $b_{1,NG}(t)$ as well as $a_{3,NG}(t)$ and $b_{3,NG}(t)$.

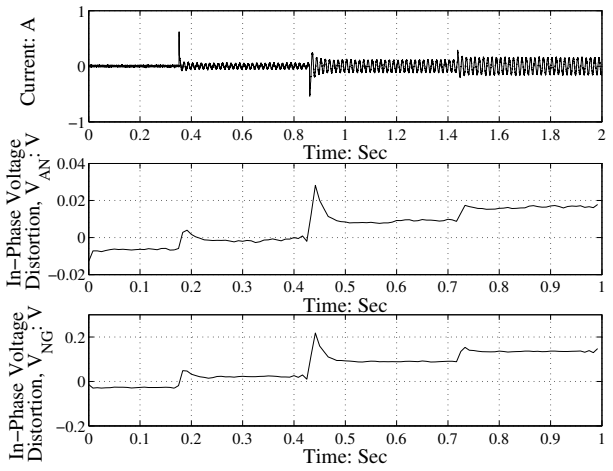

Fig. 10. The measured current and estimated spectral coefficients $a_{1,AN}(t)$ and $a_{1,NG}(t)$ as a three-way incandescent lamp progresses through its various states.

For a number of different loads, the estimated spectral coefficients of the neutral-to-ground voltage are also reliable and repeatable indicators of load operation. For example, Fig. 10 shows estimates of $a_{1,NG}(t)$ and $a_{1,AN}(t)$ that were computed during three consecutive incandescent light bulb starts. During a single start, the magnitudes of both estimates display a significant initial increase, as a considerable amount of current is drawn by the bulb. As the filament inside the bulb heats, the peaks of the estimates of $a_{1,NG}(t)$ and $a_{1,AN}(t)$ decrease as expected.

There are several potential advantages to be derived by measuring the spectral content of both the line-to-neutral voltage and the neutral-to-ground voltage. For instance, experimental measurements performed in two different locations have shown that in steady state, the typical amplitude of the line-to-neutral voltage is on the order of several volts. By comparison, the fundamental component of the voltage measured between the phase conductor and the neutral wire has a nominal RMS value of 120V. As a result, we have found that it is somewhat easier to detect changes in the neutral-to-ground voltage, especially at the higher order harmonic frequencies. As an example, consider Fig. 11, which displays estimates of the spectral coefficients $a_{1,NG}(t)$ and $a_{3,NG}(t)$ during the starting period of a rapid-start fluorescent lamp. In particular, note that the estimate of $a_{3,NG}(t)$ has a shape that

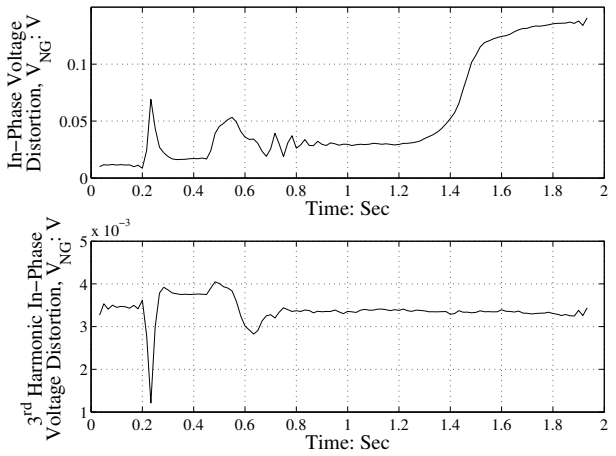

Fig. 11. Estimates of $a_{1,NG}(t)$ and $a_{3,NG}(t)$ during the starting period of a rapid-start fluorescent lamp.

is remarkably similar to that of the spectral envelope of the third harmonic current (see [3] for an example).

Additionally, the neutral-to-ground voltage helps to localize the identification problem. For example, homes in the United States are required to have their neutral conductor tied to earth ground at the utility service entrance [10]. As a result, any time that a load inside the monitored home is connected to the utility, the spectral content of the neutral-to-ground voltage tends to increase and the spectral content of the line-to-neutral voltage tends to decrease. By comparison, if a load is connected at a nearby home that is fed by the same distribution transformer, the spectral coefficients of both the neutral-to-ground voltage and the line-to-neutral voltage tend to decrease. During limited field testing of the prototype system, the use of the neutral-to-ground voltage has been found to aid in the load identification process.

IV. Load Identification

Once the spectral envelope estimates have been created by the preprocessor, they are passed to a software module that uses observed transient patterns in order to identify the operation of individual loads. The identification procedure used here, which is based on the methods used in a traditional NILM, proceeds in several steps [3]. First, incoming data from the preprocessor is searched to find any events. If an event is located, the identification software attempts to match the data surrounding the event to templates known as exemplars. Each known transient event has its own exemplar, which consists of one or more sections that characterize the given transient. Several parameters are varied in order to match an exemplar to the incoming data. Those parameters include a gain that applies to all sections in the exemplar, an offset associated with each individual section, and a delay or advance for each section that is defined relative to the time when the event was detected. As shown in the examples that follow, individual sections do not need to consist of an uninterrupted series of

data points; rather, a single section can have multiple regions of support. Each time an event is detected, the corresponding data is compared against each exemplar in a known library. The exemplar with the best fit to the incoming data is accepted as a match.

The event detector software employed in the prototype system searches for events using both the spectral coefficients $a_{k,AN}(t)$ and the spectral coefficients $a_{k,NG}(t)$. Individual events are detected using a change-of-mean scheme. In particular, events are signalled when the absolute value of the difference between the input data and a low pass filtered version of the input data exceeds a preset threshold. Once an event has been detected, the identification software fits exemplars to the incoming data. For a short period following a single detection, any new events are ignored.

The procedure used to fit exemplars to data is based on the methods employed in [3]. The fitting process is performed in an approximate manner as a series of decoupled estimation problems. Each section in the exemplar is characterized by both an index t that provides the offset relative to the first section of the exemplar and by a shape vector s that defines the qualitative shape of the section. Assuming that an event was detected at time t_e and that the spectral envelope data on the channel associated with the given section is contained in the vector d, that section of the exemplar is matched by solving the following least-squares problem:

$$\begin{pmatrix} 1 & s \end{pmatrix} X = \tag{4}$$

$$\begin{pmatrix} d[t_e+t-k] & d[t_e+t-k+1] & \dots & d[t_e+t+k] \end{pmatrix},$$

where k is a constant that defines the transient window. Note that each of the entries on the right hand side of Eq. 4 is a column vector whose first entry is specified by the given index and that X is a matrix with $2k+1$ columns and two rows. The final shift of a given section of the exemplar is determined by finding the column r of the right hand side and the corresponding column x of the matrix X that provides the best fit. This procedure is performed for each section of the exemplar, yielding a set of vectors r_k and x_k. As a final step, the entire exemplar is fit to the data by determining an appropriate gain constant to apply to all sections. This is done by solving the following least-squares problem:

$$\begin{pmatrix} s_1 \\ \vdots \\ s_N \end{pmatrix} a = \begin{pmatrix} r_1 - x_1[1] \\ \vdots \\ r_N - x_N[1] \end{pmatrix}, \tag{5}$$

where s_k is the shape vector corresponding to the $k'th$ of the N sections of the exemplar.

The data plotted in Fig. 12 demonstrates the success of the load identification procedure using the voltage-only preprocessor. The upper trace in that figure is the estimate of the spectral coefficient $a_{1,AN}(t)$, and the bottom trace is the estimate of the spectral coefficient $a_{1,NG}(t)$. As indicated by the exemplar fits, the transient event detector correctly classified both observed events as lamp starts. During the course of our preliminary testing, we have successfully identified numerous other loads, including induction motors, fluorescent lamps, and personal computers.

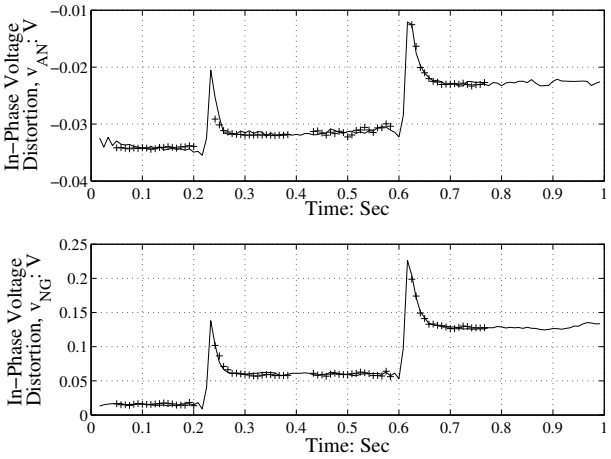

Fig. 12. Demonstration of the transient event detection software for two consecutive incandescent light bulb starts. The upper trace is the estimate of $a_{1,AN}(t)$ and the bottom trace is the estimate of $a_{1,NG}(t)$ over the same period. Overlaid atop both traces are the exemplars that were fit to each observed event. Note that two exemplars are shown in each plot, and that each exemplar consists of two regions of support (i.e. there is one region of points before each start and another region of points after each start).

The prototype system described here can track the behavior of loads whose operation is more sophisticated than that of the simple on-off devices described thus far. Specifically, the prototype system has shown an ability to be able to track the operation of loads whose behavior follows a finite-state machine (FSM) model. Fig. 13 shows state diagrams for two example FSM-type loads that have been tracked using this system [11]. As an example, consider Fig. 10, which displays estimates of $a_{1,AN}(t)$ and $a_{1,NG}(t)$ as a three-way lamp transitions from its off state to its high power state. In order to track such loads automatically, future incarnations of this system will include software similar to that described in [11].

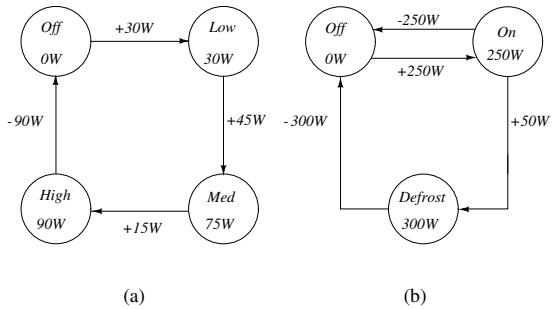

Fig. 13. Two finite-state appliance models: (a) a three-way incandescent lamp and (b) a refrigerator with a defrost state. The power levels written inside each state correspond to the nominal power drawn by the load during steady operation in that state. The power levels written next to each arc correspond to the amount by which the steady state power drawn by the load must change in order to make the prescribed state transition.

V. Conclusion

This paper has demonstrated a new monitoring system for tracking individual load operation on an aggregate power service using only voltage measurements, i.e. with no current sensor. The system described in this paper opens the door to easy, inexpensive, and accurate load monitoring. Installation of the monitor is as easy as plugging in an appliance. A variety of demand-side power management features could be incorporated directly into loads made "aware" of their operating environment through the inclusion of this load monitor.

The operational examples included in this paper are a subset taken from the many tests that have been performed using the prototype system. The prototype system balances analog and digital processing in order to provide an inexpensive means to detect small load power transients. To date, the complete system has been able to identify nearly all load events observed during testing periods. Current results indicate that an improved transient event detector would allow this system to achieve performance levels rivaling those of a standard NILM for loads with steady state power levels above $50\mathrm{W}$. Performance in this range implies that this system would be able to identify nearly all household appliances.

Acknowledgment

This research was funded in part by the CMI Program at MIT and by the Grainger Foundation. The authors gratefully acknowledge the valuable advice provided by Professor Andy Woods at Cambridge University.

References

[1] A. Fanara, "ENERGY STAR®: A strategy to encourage improved efficiency of power supplies," in *Proc. 19th Applied Power Electronics Conf. and Expo.*, 2004, pp. 24–30.

[2] S.B. Leeb, S.R. Shaw, and J.L. Kirtley, "Transient event detection in spectral envelope estimates for nonintrusive load monitoring," *IEEE Trans. Power Delivery*, vol. 10, no. 3, pp. 1200–1210, July 1995.

[3] S. Shaw, "System identification and modeling for nonintrusive load diagnostics," Ph.D. dissertation, Massachusetts Institute of Technology, Cambridge, MA, 2000.

[4] S.R. Shaw and C.R. Laughman, "A kalman-filter spectral envelope preprocessor," submitted for publication in *IEEE Trans. Instrum. Meas*, Feb. 26. 2004.

[5] S.R. Sanders, J.M. Noworolski, X.Z. Liu, and G.C. Verghese, "Generalized averaging method for power conversion circuits," *IEEE Trans. Power Electron.*, vol. 6, no. 2, pp. 251–259, Apr. 1991.

[6] A. de Oliveira, J.C. de Oliveira, J.W. Resende, and M.S. Miskulin, "Practical approaches for AC system harmonic impedance measurements," *IEEE Trans. Power Delivery*, vol. 6, no. 4, pp. 1721–1726, Oct. 1991.

[7] S.R. Shaw, C.R. Laughman, S.B. Leeb, and R.F. Lepard, "A power quality prediction system," *IEEE Trans. Ind. Electron.*, vol. 47, no. 3, pp. 511–517, June 2000.

[8] W.C. Beattie and S.R. Matthews, "Impedance measurement on distribution networks," in *Proc. 29th Universities Power Engineering Conf.*, Sept. 1994, pp. 117–120.

[9] A. Oury, R. Bergeron, and A. Laperrière, "Source impedances of the Canadian distribution systems (residential and industrial)," in *Proc. 14th International Conf. and Expo. on Electrity Distribution*, vol. 2, June 1997, pp. 34/1–34/8.

[10] *National Electrical Code*, National Fire Protection Association, Quincy, MA, 1999.

[11] G. W. Hart, "Nonintrusive appliance load monitoring," *Proc. IEEE*, vol. 80, no. 12, pp. 1870–1891, Dec. 1992.